

Identification of Mouse Histone Deacetylase 1 as a Growth Factor-Inducible Gene

STEFAN BARTL,¹ JAN TAPLICK,¹ GERDA LAGGER,¹ HARALD KHIER,¹
KARL KUCHLER,² AND CHRISTIAN SEISER^{1*}

*Institute of Molecular Biology¹ and Institute of Molecular Genetics,² University of Vienna,
Vienna Biocenter, A-1030 Vienna, Austria*

Received 22 April 1997/Returned for modification 27 May 1997/Accepted 16 June 1997

Reversible acetylation of core histones plays an important role in transcriptional regulation, cell cycle progression, and developmental events. The acetylation state of histones is controlled by the activities of acetylating and deacetylating enzymes. By using differential mRNA display, we have identified a mouse histone deacetylase gene, HD1, as an interleukin-2-inducible gene in murine T cells. Sequence alignments revealed that murine HD1 is highly homologous to the yeast *RPD3* pleiotropic transcriptional regulator. Indirect immunofluorescence microscopy proved that mouse HD1 is a nuclear protein. When expressed in yeast, murine HD1 was also detected in the nucleus, although it failed to complement the *RPD3* deletion phenotype. HD1 mRNA expression was low in G₀ mouse cells but increased when the cells crossed the G₁/S boundary after growth stimulation. Immunoprecipitation experiments and functional in vitro assays showed that HD1 protein is associated with histone deacetylase activity. Both HD1 protein levels and total histone deacetylase activity increased upon interleukin-2 stimulation of resting B6.1 cells. When coexpressed with a luciferase reporter construct, HD1 acted as a negative regulator of the Rous sarcoma virus enhancer/promoter. HD1 overexpression in stably transfected Swiss 3T3 cells caused a severe delay during the G₂/M phases of the cell cycle. Our results indicate that balanced histone acetylation/deacetylation is crucial for normal cell cycle progression of mammalian cells.

In eukaryotic cells, histones are essential for the packaging of DNA. The smallest unit of genome organization, the nucleosome, consists of 146 bp of DNA wrapped around an octamer of core histones (H2A, H2B, H3, and H4). These core histones are the target of different modifications including phosphorylation, methylation, ubiquitination, and acetylation, of which the latter is probably the most extensively studied. Dynamic acetylation and deacetylation of lysine residues within the highly conserved N-terminal part of core histones seem to be necessary for a number of crucial nuclear events including transcriptional silencing (11), replication (4, 19, 49, 50, 64), and DNA repair (19, 51, 58). However, the exact biological function of these modifications is still unknown (10, 35, 36, 72).

One way to study core histone acetylation is the identification of the involved acetylating and deacetylating enzymes. During the last few years, histone acetyltransferases and histone deacetylases have been characterized and partially purified from yeast, the slime mold *Physarum*, plants, and mammals (3, 6, 9, 18, 21, 23, 26, 37–39, 44, 66). A yeast B-type acetyltransferase with specificity for lysine 12 was recently identified by a genetic approach (32). A nuclear A-type histone acetyltransferase of *Tetrahymena* was shown to be homologous to the yeast transcriptional regulator Gcn5 (13). Recently, isolation by affinity chromatography led to the identification of a human histone deacetylase as a homolog of the yeast transcription modulator *RPD3* (65). Rpd3 and a Rpd3-related protein have been localized in two distinct yeast histone deacetylase complexes (54).

Specific antibodies recognizing certain acetylated histone

isoforms have been shown to be very useful tools for investigating the relationship between chromatin structure and histone acetylation. Probing *Drosophila* salivary gland polytene chromosomes with these antibodies revealed a characteristic acetylation pattern for specific lysine residues throughout the genome. In particular, histone H4 in heterochromatin regions was less acetylated at lysines 5 and 8 but hyperacetylated at lysine 12 (67). In contrast to all other chromosomes, the inactive mammalian X chromosome is largely unlabelled by specific antibodies directed against the acetylated form of lysines 5, 8, 12, and 16 at histone H4 (27). Immunoprecipitation of chromatin fragments from human HL-60 cells with similar antibodies confirmed that the heterochromatin contains underacetylated forms of H4, although the acetylation of histone H4 was not correlated with transcriptional activity (47).

Another important step toward the understanding of the role of histone acetylation was the identification of specific inhibitors of histone deacetylases (12; for a review, see reference 77). Trichostatin A, a fungistatic antibiotic, has been shown to induce differentiation in erythroleukemia cells (78), to block the development of *Xenopus* and starfish embryos (2), to induce the expression of different genes (5, 20, 25, 43), and to arrest normal fibroblasts in the G₁ or G₂ phase of the cell cycle (76). Furthermore, trichostatin A and trapoxin, another specific inhibitor of histone deacetylases, also have the potential to revert the phenotype of oncogene-transformed fibroblasts (17, 62, 75).

In this publication, we report the identification of a murine histone deacetylase gene, HD1, as a homolog of the yeast transcription coregulator *RPD3*. HD1 mRNA levels and HD1 protein levels are low in interleukin-2 (IL-2)-deprived T cells but rise severalfold in response to IL-2 stimulation. While endogenous HD1 levels vary in different mouse cell lines without obvious consequence on cell proliferation, induced over-

* Corresponding author. Mailing address: Institute of Molecular Biology, Vienna Biocenter, Dr. Bohr-Gasse 9, A-1030 Vienna, Austria. Phone: 431 795 15/2630. Fax: 431 798 62 24. E-mail: cs@mol.univie.ac.at.

expression of HD1 impaired the cell cycle progression of transfected Swiss 3T3 cells. We propose that cell-specific optimal histone deacetylase activity levels are needed for undisturbed cell growth and proper chromatin function.

MATERIALS AND METHODS

Cell culture and media. B6.1 is an IL-2-dependent cytolytic mouse cell line (56, 71). B6.1 cells were grown in Dulbecco's modified Eagle's medium supplemented with 5% heat-inactivated fetal calf serum, 50 mM β -mercaptoethanol, 10 mM L-glutamine, and 100 U of recombinant human IL-2 (gift of M. Nabholz, ISREC, Lausanne, Switzerland) per ml. The cell lines Swiss 3T3, C127, COP-8, and F9 were kept in Dulbecco's modified Eagle's medium supplemented with 10% fetal calf serum. Swiss 3T3 cells were growth arrested by reducing the serum concentration in the culture medium to 0.2% for 72 h and restimulated to enter the cell cycle by using fresh medium containing 20% fetal calf serum. Growth arrest and stimulation were routinely controlled by fluorescence-activated cell sorter (FACS) analysis with a Partec PAS-II sorter. Centrifugal elutriation of exponentially growing Swiss 3T3 cells (usually 3×10^8 cells) was performed with Beckman elutriation equipment.

Retroviral infection and transfection of mammalian cells. The *EcoRI-PstI* fragment of the mouse HD1 cDNA was subcloned into Bluescript KS (Stratagene), resulting in the plasmid pKSHD1cod. The stop codon of the murine HD1 coding sequence was replaced by a *BamHI-SacI* linker by standard PCR methods, and an oligodeoxynucleotide encoding the *c-myc* epitope EEQKLI SEEDLLRKR (16) was cloned in frame into the generated sites. The corresponding in vitro transcription/translation product was recognized by the 9E10 antibody (Oncogene Science) directed against the *c-myc* tag (data not shown). The cDNA fragment coding for *c-myc* tagged HD1 was cloned into the retroviral vector pBABE-Puro (45). High-titer retroviral supernatants were generated by transient transfection of BOSC23 cells and used to infect Swiss 3T3 cells as described previously (48). Infected cells were selected for 2 days in culture medium supplemented with 2.5 μ g of puromycin per ml and analyzed for expression of epitope-tagged HD1 protein by immunofluorescence and immunoblotting.

For transient expression of HD1 from the cytomegalovirus promoter, the coding region of the murine HD1 cDNA was cloned into the mammalian expression vector pCIneo (Promega). For inducible expression, the coding region of the HD1 cDNA was cloned into the pMAMneo vector (Clontech, Palo Alto, Calif.) under the transcriptional control of the mouse mammary tumor virus long terminal repeat in an attempt to confer glucocorticoid inducibility to the cDNA. Cultures of Swiss 3T3 cells were transfected with the HD1-encoding vector or the empty plasmid by the Lipofectin method (Gibco) as recommended by the supplier. About 24 h after transfection, cells were selected in culture medium containing 400 μ g of G418 per ml. Individual resistant clones were isolated 10 days later and passaged into stable cell lines. Two cell lines with moderate HD1 overexpression (represented by the cell line HD1-A) and a strongly overexpressing cell line designated HD1-B were further characterized.

Indirect immunofluorescence. Infected Swiss 3T3 cells expressing epitope-tagged HD1 were fixed with 3% paraformaldehyde and permeabilized with 0.5% Triton X-100. The *c-myc*-tagged proteins were detected with monoclonal antibody 9E10 and visualized with a Texas Red-conjugated anti-mouse immunoglobulin G IgG secondary antibody (Accu-Specs) in a Zeiss Axiovert 135TV microscope.

Yeast methods. The yeast strains W303-1A (*MATa leu2-3,112 ura3-1 trp1-1 his3-11,15 ade2-1 can1-100*) (53) and YJT1 (*MATa leu2-3,112 ura3-1 trp1-1 his3-11,15 ade2-1 can1-100 rpd3 Δ ::HIS3*) (this study) were used. Strain M833 (*MATa ura3-52 trp1 Δ 1 his3-200 leu2-1 trk1 Δ rpd3 Δ ::HIS3*), and M835 (*MATa ura3-52 trp1 Δ 1 his3-200 leu2-1 trk1 Δ*) were generously provided by R. Gaber (70). Standard media and techniques in yeast work were used as previously described (52). For phenotype determination, yeast strains were spotted and grown on cycloheximide agar plates as described previously (70).

Plasmid construction for yeast expression. For constitutive expression of murine HD1 in yeast, a *SalI-SacI* fragment of pKSHD1 containing the HD1 cDNA was cloned into pAD4D (8), resulting in plasmid pADHD1. The construct for expression of *c-myc*-tagged HD1 was obtained by cloning the *SalI-SacI* insert of pSVLHD1myc into pAD4D, yielding pADHD1myc. Yeast *RPD3* was amplified by PCR with the primers 5'-GCG TCG ACC GTG GCT ACA ACT CGA TAT C-3' and 5'-CGA GCT CCA ATA GAA TTC ATT GTC ATG C-3'. The PCR product was digested with *SalI* and *SacI* and cloned into a *SalI-SacI*-opened pAD4D to give pADRPD3. Mouse HD1 cDNA and the yeast *RPD3* gene have a common *NcoI* site within the coding sequence at about equivalent positions (mouse HD1 at position 551, yeast *RPD3* at position 783). To construct HD1:*RPD3* chimeras, the *SalI-NcoI* fragment of pADHD1 was replaced by the corresponding *SalI-NcoI* fragment of pADRPD3. This construct (pADRPD3HD1) encodes a hybrid protein with the N-terminal 189 amino acids of yeast *Rpd3* and the C-terminal 245 residues of mouse HD1. The complementary constructs were obtained by cloning the *SalI-NcoI* fragments of pADHD1 and pADHD1myc into pADRPD3 partially digested with *NcoI* and *SalI* (pADRPD3HD1 and pADRPD3HD1myc, respectively). Indirect immunofluorescence to detect the epitope-tagged mouse protein in yeast was done as previously described (15). To

disrupt the *RPD3* gene in *Saccharomyces cerevisiae*, plasmid pJJRPD3 was constructed as follows. Two fragments of *RPD3* corresponding to bp 405 to 805 and 815 to 1197 were cloned via *EcoRI-SacI* and *Clal-XbaI* digestion, respectively, into pJJ215 (28). Plasmid pJJRPD3 was digested with *EcoRI-SalI* and used to transform strain W303-1A. Correct disruption of the *RPD3* gene in the genome of the resulting strain YJT1 was confirmed by PCR and Southern blot hybridization.

Differential mRNA display. Differential mRNA display was performed by the method originally described by Liang and Pardee (34). Cytosolic RNA was extracted from B6.1 cells after IL-2 deprivation and restimulation for 16 h as described previously (56). Following reverse transcription, PCR was performed with five different arbitrary primers. The HD1-specific PCR product was obtained in three independent approaches with the primer 5'-GGT CCC TGA C-3'. The fragment was reamplified by PCR and cloned into the pGEM-T vector (Promega).

Isolation of HD1 full-length cDNA and RNA methods. A mouse cDNA library prepared from growth-induced Swiss 3T3 cells (generous gift of R. Hofbauer) was screened with the subcloned clone 16 DNA fragment by standard procedures. Cytosolic RNA was extracted as previously described (56). Total RNA from mouse tissues was isolated by the GTC method (RNAgens total RNA isolation kit; Promega) as specified by the manufacturer. Northern blot hybridization was done by the sandwich method (63) with radiolabeled probes such as the full-length HD1 cDNA fragment, the 0.3-kb *HhaI-EcoRI* fragment of mouse β_2 -microglobulin cDNA, the 1.2-kb mouse thymidine kinase cDNA (24), and an oligonucleotide complementary to nucleotides 3046 to 3063 of the murine 28S rRNA.

Preparation of a polyclonal HD1 antiserum. The *BglII-PstI* fragment of HD1 cDNA was cloned into the *BamHI-PstI*-linearized plasmid pQE32 (Qiagen). The resulting open reading frame encodes a N-terminal truncated version of murine HD1 (amino acids 53 to 482) preceded by a histidine tag. The fusion protein was expressed in *Escherichia coli* PR13Q and purified by nickel column chromatography as described by the supplier (Qiagen). The recombinant protein was used to immunize rabbits by standard immunological techniques (Eurogentec, Seraing, Belgium).

Western blot analysis. Whole-cell extracts of mouse cells and yeast cells were prepared as described in references 1 and 15, respectively. Western blot analysis of endogenous and *c-myc*-tagged HD1 was performed as previously described (63). Detection was performed by enhanced chemiluminescence (NEN-Dupont).

Histone deacetylase assay and immunoprecipitation of HD1-associated activity. Histone deacetylase enzyme activity in whole-cell extracts was determined as described by Lechner et al. (33). Equal amounts (10 μ g) of protein were incubated with 10 μ l of [3 H]acetate-labeled chicken erythrocyte histones in a total volume of 50 μ l for 1 h at 30°C. The reaction was stopped by the addition of 36 μ l of 1 N HCl-0.4 M acetate and 0.8 ml of ethyl acetate. After centrifugation at $8,400 \times g$ for 5 min, a 600- μ l aliquot of the organic phase was counted in 3 ml of liquid scintillation cocktail. To determine the histone deacetylase activity in immunoprecipitates, whole-cell extracts were incubated with 1 μ l of serum and 20 μ l of protein G-Sepharose bead suspension (10% [vol/vol]; Pharmacia) for the tagged HD1 protein or 20 μ l of protein A-Sepharose bead suspension (10% [vol/vol]; Pharmacia) for the endogenous HD1 protein. After three washes with the extraction buffer, the beads were resuspended in 50 μ l of HD buffer (65) and 20- μ l aliquots were examined as described previously (33).

Luciferase activity assay. Plasmid pRSVluc, which contains the firefly luciferase gene under control of the Rous sarcoma virus (RSV) long terminal repeat, was transiently expressed in the human lung carcinoma cell line A549 (14). Triplicate transfections with Lipofectin (Gibco) were performed in 24-well plates with 0.5 μ g of pRSVluc together with (i) 1 μ g of pCIneo, (ii) 0.5 μ g of pCIneo and 0.5 μ g of pCIneoHD1, or (iii) 1 μ g of pCIneoHD1. These experiments demonstrated that both HD1 protein levels and enzyme activity increased with the amount of transfected pCIneoHD1 plasmid. After 24 h, the cells were lysed and the extracts were analyzed by the luciferase reporter gene assay (Berthold Detection Systems, Pforzheim, Germany) with the AutoLumat LB953 system (EG&G; Berthold, Bad Wildbad, Germany) under the conditions recommended by the supplier.

Nucleotide sequence accession number. The mouse HD1 cDNA sequence has been deposited in the EMBL nucleotide sequence database under accession no. X98207.

RESULTS

Isolation and sequence of the mouse HD1 cDNA. The cytolytic mouse T-cell line B6.1 was previously used as a model system to study growth-dependent gene expression (56). B6.1 cells arrest in G_0 when deprived of IL-2 for 34 h, but they can be restimulated to cycle by addition of fresh medium containing recombinant IL-2 (71). To identify novel growth-regulated genes in this cell system, we have used differential mRNA display (34). We have isolated several PCR products that showed a reproducible IL-2-dependent difference in their

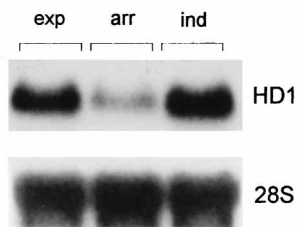


FIG. 1. Differential expression of clone 16 mRNA in response to IL-2. Northern blot analysis of exponentially growing B6.1 cells (exp), resting B6.1 cells (arr), and cells restimulated with IL-2 for 16 h (ind) was performed. The membrane was sequentially hybridized with the reamplified PCR fragment of clone 16 and a probe for the 28S rRNA.

abundance. Northern analysis revealed that cDNA fragment 16 recognized a 2.2-kb mRNA with strongly reduced expression in IL-2-deprived B6.1 cells (Fig. 1). With this cDNA fragment as the probe, a full-length cDNA clone (clone 16) was

isolated from a cDNA library generated with poly(A)⁺ RNA from growth-stimulated Swiss 3T3 mouse fibroblasts (a generous gift of R. Hofbauer). Sequence analysis showed that the cDNA was 1,977 bp long with an open reading frame of 1,449 nucleotides potentially encoding a 482-residue protein (Fig. 2). The predicted molecular mass of 55 kDa was confirmed in vitro by transcription-translation experiments, since reticulocyte lysates gave a protein product of the expected size (data not shown).

Comparison with nucleotide sequences in the available databases revealed that HD1 is almost identical to a recently isolated human histone deacetylase (65). The polypeptide encoded by fragment 16 differs from human HD1 in only 3 amino acid residues, all of which are conservative exchanges (Fig. 3). Therefore, it is reasonable to conclude that we have cloned the mouse homolog of human HD1 as an IL-2-inducible gene. Moreover, HD1 displayed a striking homology (58% identity on the amino acid level) to the yeast protein Rpd3 (Fig. 3).

GCCGGGCGGCGAGCAAGATGGCGCAGACTCAGGGCACCAAGAGGAAAGTCTGTTACTACTACGACGGGGATGTTGGAACTACTATTATG	90
M A Q T Q G T K R K V C Y Y Y D G D V G N Y Y Y G	25
GACAAGGGCACCCCATGAAGCCTCACCGAATCCGCATGACTCACAAATTTGCTGCTCAACTATGGTCTCTACCGAAAAATGGAGATCTACC	180
Q G H P M K P H R I R M T H N L L L N Y G L Y R K M E I Y R	55
GCCCTCACAAAGCCAATGCTGAGGAGATGACCAAGTACCACAGTATGACTACATTAATTCCTGCGTTCATTCGCCAGATAACATGT	270
P H K A N A E E M T K Y H S D D Y I K F L R S I R P D N M S	85
CTGAATACAGCAAGCAGATGCAGAGATTCAATGTTGGTGAGGACTGTCGGTATTTGATGGCTTGTGAGTTCTGTCAGTTGTCCACGG	360
E Y S K Q M Q R F N V G E D C P V F D G L F E F C Q L S T G	115
GAGGCTCTGTGCGAAGTGTGTGAAGCTTAATAAGCAGCAGACGGACATCGCTGTGAAC TGGGCTGGGGCCTGCACCATGCAAGAAGT	450
G S V A S A V K L N K Q Q T D I A V N W A G G L H H A K K S	145
CTGAAGCATCCGGCTTCTGTTACGTCATGACATCGTCTTGGCCATCCTGGAACTGCTAAAGTACCACCAGGGTGTCTATATTGACA	540
E A S G F C Y V N D I V L A I L E L L K Y H Q R V L Y I D I	175
TTGATATTCACCATGGCGATGGCGTGGAAAGGGCCTTCTATACACAGACCGGGTCACTGACTGTGCTCTTTCATAAATACGGAGAGTACT	630
D I H H G D G V E E A F Y T T D R V M T V S F H K Y G E Y F	205
TCCAGGAACTGGGGACCTACGGGACATGGGGCTGGCAAAGGCAAGTACTATGCTGTGAAC TACCCACTGCAGACGGCAITTGACGACG	720
P G T G D L R D I G A G K G K Y Y A V N Y P L R D G I D D E	235
AATCCTATGAAGCCATCTTTAAGCCAGTCAATGTCCTCAAGTAAATGGAGATGTTCCAGCCTAGTGCAGTGGTCTTACAGTGTGGCTCAGATT	810
S Y E A I F K P V M S K V M E M F Q P S A V V L Q C G S D S	265
CCCTGTCTGGGGACCGGTTAGGTTGCTTCAATCTGACCATCAAAGCACGCAAGTGTGTGGAGTTCGTGAAGAGTTTCAGTTGCCCA	900
L S T G D R L G C F N L T I K G H A K C V E F V K S F N L P M	295
TGCTGATGCTGGGAGGAGTGGCTACACCATCCGGAATGTTGCTCGTCTGGACTTACGAAACAGCGGTGGCCCTGGACACAGAGATCC	990
L M L G G G G Y T I R N V A R C W T Y E T A V A L D T E I P	325
CTAATGAGCTGCCCTACAATGACTACTTTGAATACTTTGGACCGGATTTCAAGCTTACATCAGCCCTTCTAACATGACCAACCAGAACA	1080
N E L P Y N D Y F E Y F G P D F K L H I S P S N M T N Q N T	355
CTAACGAGTACCTGGAGAAGATCAAGCAGCTCTCTTTGAGAACTTGGAGATGTGCCCATGCCCTGGGGTCCAGATGCAGGCCATCC	1170
N E Y L E K I K Q R L F E N L R M L P H A P G V Q M Q A I P	385
CTGAGGACGCCATCCCGAAGAGATGGGGATGAAGATGAGGAGGACCTGACAAACGCATCTCCATCTGCTCCTCTGATAAACGCATTG	1260
E D A I P E E S G D E D E E D P D K R I S I C S S D K R I A	415
CCTGTGAGGAAGAGTTCTCGGACTCAGATGAGGAGGGAGAAGGTGGTTCGCAAGAACTCTTCTAACTTCAAAAAGCCAAAAGAGTTAAAA	1350
C E E E F S D S D E E G E G G R K N S S N F K K A K R V K T	445
CAGAGGATGAGAAGAGAAAGATCCTGAAGAGAAAAAAGTACAGAGAAGAGAAAACCAAGGAGGAGAAGCCAGAAGCCAAAGGGG	1440
E D E K E K D P E E K K E V T E E E K T K E E K P E A K G V	475
TCAAAGAAGAGGTCAAGTTGGCCTGAGCAAGGTCTGCAGCCCATCTTCTCCCAAGTTCCTCACTCTCCCTCAACTTCTCAGATTTTAT	1530
K E E V K L A	482
ATTTTCTATTCCTCTGTGATTATATATAAAATATATAACTATAACGTCCTCCAGGGACAGAGCACAGGGCAGTGGTCTAGGAGGGCTC	1620
TTCCCAGAGCGACTTGTCCATCCTGCCACCCCTCCCTCCCTTTGCGTGGGAAAAAACAACCCAGAAAGAGAAAATCCTGAACT	1710
GCCAAGTGCCTGCTTAGGAGCTCTGCTAAGATGCCCTGTTAAACTTTTAGGAGGGTCTGGGTCTTTTTCAGGCTTGGGTAATAGCAGC	1800
CATTTTTAGATTGGTCTGTTTATATCTCCACCCATCTTTGGGCAACAAAAAATTTATATTGCCCTGTCTTCCCAATCTGTAGG	1890
GTTGGAGTTGATAGCTAGCTTCTTTTGGAGATATTTTCAATTTTGTGAAACTCTTTGTAATAAACAGCTCATTTCTATACCCCTCA	1977

FIG. 2. Nucleotide sequence and deduced amino acid sequence of mouse HD1. The putative polyadenylation signal is underlined.

```

1 MAQTQG-----T-RRKVCYYYDGDVGNYYYGQGHMPKPHRIRMTHNLLLNGLYRKMETIRPHKAN HHD1 . PRO
1 MAQTQG-----T-KRKVCYYYDGDVGNYYYGQGHMPKPHRIRMTHNLLLNGLYRKMETIRPHKAN MHD1 . PRO
1 MAYSQG-----GGKKVCYYYDGDIGNYYYGQGHMPKPHRIRMTHNLLLNGLYRKMETIRPHKAT MRPD3 . PRO
1 MVVEATPFDPITVKPSDKRRVAIFYDADVGNVYAGAGHPMKPHRIRMAHSLIMNYGLYKMEIYRAKPAT YRPD3 . PRO

61 AEEMTKYHSDDYIKFLRSIRPDNMSEYSKQMORFNVGEDCPVFDGLFEFCQLSTGGSVASAVKLNKQQT D HHD1 . PRO
61 AEEMTKYHSDDYIKFLRSIRPDNMSEYSKQMORFNVGEDCPVFDGLFEFCQLSTGGSVASAVKLNKQQT D MHD1 . PRO
62 AEEMTKYHSDEYIKFLRSIRPDNMSEYSKQMORFNVGEDCPVFDGLFEFCQLSTGGSVAGAVKLNKQQT D MRPD3 . PRO
71 KQEMCQFHITDEYIDFLSRVTPDNLEMPKRESVKFNVGDDCPVFDGLYEYCSISGGSGMEGAARLNRGKCD YRPD3 . PRO

131 IAVNWAGGLHHAHKSEASGFCYVNDIVLAI LLELLKYHQRVLYIDIDIHHGDGVVEAFYTTDRVMTVSFHK HHD1 . PRO
131 IAVNWAGGLHHAHKSEASGFCYVNDIVLAI LLELLKYHQRVLYIDIDIHHGDGVVEAFYTTDRVMTVSFHK MHD1 . PRO
132 MAVNWAGGLHHAHKSEASGFCYVNDIVLAI LLELLKYHQRVLYIDIDIHHGDGVVEAFYTTDRVMTVSFHK MRPD3 . PRO
141 VAVNYAGGLHHAHKSEASGFCYLNDIVLGI IELLRYHPRVLYIDIDVHHGDGVVEAFYTTDRVMTCSFHK YRPD3 . PRO

201 YGEYFFPGTGLRDI GAGKGYAVNYP LRDGIDDES YEAIKFPVMSKVMEMFQPSAVVLQCGSDSLSGDR HHD1 . PRO
201 YGEYFFPGTGLRDI GAGKGYAVNYP LRDGIDDES YEAIKFPVMSKVMEMFQPSAVVLQCGSDSLSGDR MHD1 . PRO
202 YGEYFFPGTGLRDI GAGKGYAVNFP MRDGI DDES YGQIFKPIISKVMEYQPSAVVLQCGADSLSGDR MRPD3 . PRO
211 YGEYFFPGTGLRDI GAGKGYAVNVP LRDGID DATYRSVFEPVIKKIMEWYQPSAVVLQCGSDSLSGDR YRPD3 . PRO

271 LGCENLTKGHAKCVFVKSFNLEMLMLGGGGYTRNVARCWTYETAVALDTEIPNELPYNDYFEYFGPD HHD1 . PRO
271 LGCENLTKGHAKCVFVKSFNLEMLMLGGGGYTRNVARCWTYETAVALDTEIPNELPYNDYFEYFGPD MHD1 . PRO
272 LGCENLTKGHAKCVFVAKTFNLLMLGGGGYTRNVARCWTYETAVALDCEIPNELPYNDYFEYFGPD MRPD3 . PRO
281 LGCENLSMEGHANCVNYSKFGIPMMVVGGGGYTRNVARCWTYETAVALDTEIPNELPYNDYFEYFGPD YRPD3 . PRO

341 FKLHISPSNMTNQNINTEYLEKIKORLFENLRMLPHAPGVQMQAIPEDAIPESGDEDEDPPDKRISICSS HHD1 . PRO
341 FKLHISPSNMTNQNINTEYLEKIKORLFENLRMLPHAPGVQMQAIPEDAIPESGDEDEDPPDKRISICSS MHD1 . PRO
342 FKLHISPSNMTNQNINTEYLEKIKORLFENLRMLPHAPGVQMQAIPEDAVHEDSGDEDEDPPDKRISIRAS MRPD3 . PRO
351 YKLSVPSNMFNVNTPPEYLDKVMNTIFANLENTKYAPSVQLNHTPRDA--EDLGDVEEDSAEAK----- YRPD3 . PRO

411 DKRIACEEFSDESEEGEGGRKNSNFKK-AKRVKTEDEKEKDPBEKKEVTEEEKTKE--EKPEAKGVK HHD1 . PRO
411 DKRIACEEFSDESEEGEGGRKNSNFKK-AKRVKTEDEKEKDPBEKKEVTEEEKTKE--EKPEAKGVK MHD1 . PRO
412 DKRIACDEEFSDESEEGEGGRNVDHKKGAKKARIEEDKKETEDKKTVDVKEEDSKDNSGEKTDPKGAK MRPD3 . PRO
413 -----DTKGGSQY--ARDLHVEHDNE----- YRPD3 . PRO

477 -EEVKLA HHD1 . PRO
477 -EEVKLA MHD1 . PRO
482 SEQLSNP MRPD3 . PRO
432 ----FY YRPD3 . PRO

```

FIG. 3. Homology comparison of human HD1, mouse HD1, mouse Rpd3, and yeast Rpd3 proteins. The sequences were aligned with the Lasergene Megalign program.

Recently, another murine homolog of Rpd3 was identified as the binding partner of the transcription factor YY1 (73). This protein shares 84% identity with mouse HD1. In addition, the coding portion of clone 16 was found to be highly homologous (80% identity at the nucleotide level) to the 3' untranslated region of the chicken proto-oncogene cDNA *c-tkl* (60). However, the potential reading frame of the 3' *c-tkl* sequence is disrupted by several frameshifts. Thus, the presence of HD1-related sequences within the *c-tkl* gene is probably due to the integration of a pseudogene.

The mammalian HD1 protein displays significant homology to a number of proteins from different organisms. In addition to a *Xenopus* Rpd3 homolog, proteins from *Bacillus subtilis*, cyanobacteria, *Caenorhabditis elegans*, and two other yeast proteins have significant homology to murine HD1 (data not shown). These results suggest that HD1 is a highly conserved protein throughout different species. Furthermore, the presence of two additional HD1-like cDNAs in the human EST database and two *RPD3*-like genes in the yeast genome point to the existence of a family of related proteins in eukaryotes.

HD1 is a nuclear protein both in yeast and in mammalian cells. Since the murine HD1 protein displays high homology to the yeast *RPD3* transcription regulator, one would anticipate that this protein is localized in the nucleus. To investigate its intracellular localization, we have expressed the murine HD1 protein with a *c-myc* epitope at its carboxy terminus in Swiss 3T3 fibroblasts. Western blot analysis with protein extracts of transfected cells showed a single band with the expected size of

about 57 kDa, while extracts from untransfected cells gave no signal at all (Fig. 4A). Indirect immunofluorescence microscopy revealed that the HD1 protein is localized predominantly to the nucleus of mammalian cells while Swiss 3T3 fibroblasts transfected with the vector alone gave no detectable signal (Fig. 4B and data not shown). In parallel, we studied the localization of the murine protein expressed in yeast cells. A *c-myc*-tagged mouse HD1 was expressed in yeast under alcohol dehydrogenase (ADH) promoter control and visualized by Western blotting and immunofluorescence. Immunoblot analysis gave a single band corresponding to a polypeptide of 57 kDa (Fig. 4A). By indirect immunofluorescence microscopy, the mouse protein was also found in the nucleus of yeast cells, suggesting that the nuclear localization signal of murine HD1 is properly recognized in yeast (Fig. 4B).

Mouse HD1 fails to complement the yeast *rdp3Δ* deletion mutant phenotype. The striking homology (Fig. 3) between yeast *RPD3* and its mammalian counterpart suggests that they may fulfill similar functions in their respective organisms. To test if the mouse HD1 homolog is able to functionally complement the yeast protein, the *RPD3* gene was disrupted in strain W303-1A. Mutant *rdp3Δ* cells show an increased sensitivity to cycloheximide and reduced expression of *STE6* as described previously (70). While expression of yeast Rpd3 from an ADH multicopy plasmid conferred cycloheximide resistance, neither wild-type mouse HD1 nor the *c-myc*-tagged version was able to complement the *rdp3Δ* phenotype (data not shown). Similar results were also obtained in *rdp3Δ* strains in a *trk1Δ* back-

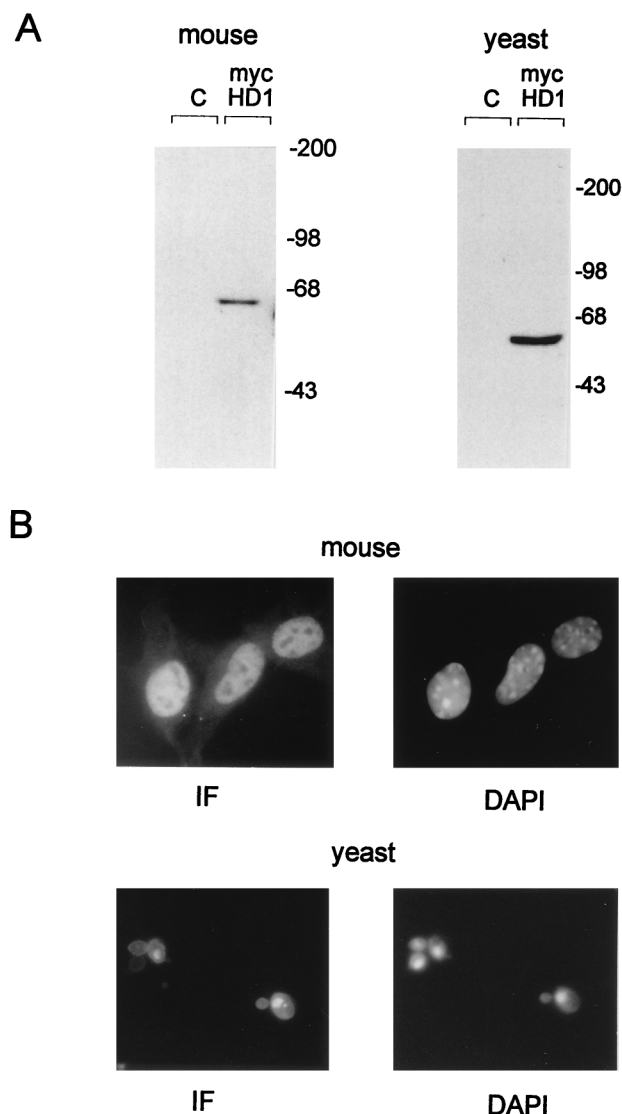


FIG. 4. Subcellular localization of mouse HD1 in Swiss 3T3 fibroblasts and yeast cells. A *c-myc*-tagged version of mouse HD1 protein was expressed in Swiss 3T3 cells and yeast cells as described in Materials and Methods. (A) Western blot analysis of murine *c-myc*-tagged HD1 protein expressed in mouse fibroblasts and in yeast cells. *c-myc*-tagged HD1 was detected with monoclonal antibody 9E10. Extracts from nontransformed yeast cells and nontransfected mouse Swiss 3T3 cells were included as controls (lanes C). (B) Indirect immunofluorescence (IF) microscopy. Epitope-tagged HD1 protein was labeled with 9E10 antibody followed by Texas red-conjugated anti-mouse immunoglobulin G. In parallel, the nuclear DNA of mouse cells and yeast cells was stained with 4',6-diamidino-2-phenylindole (DAPI).

ground (70). Chimeric hybrid constructs encompassing the N-terminal half of the yeast Rpd3 protein and the C-terminal part of the murine HD1 enzyme and vice versa also failed to increase the resistance to the cycloheximide.

Growth-regulated expression of mouse HD1 mRNA in B6.1 cells. To elucidate the kinetics of mouse HD1 mRNA induction, B6.1 cells were deprived of IL-2 for 34 h and restimulated with the lymphokine. Northern analysis showed that HD1 mRNA expression was very low in resting B6.1 cells but started to rise after a 12-h induction with IL-2 and reached ninefold-higher levels after a 24-h treatment with the lymphokine (Fig. 5A). Additional experiments showed that HD1 mRNA expres-

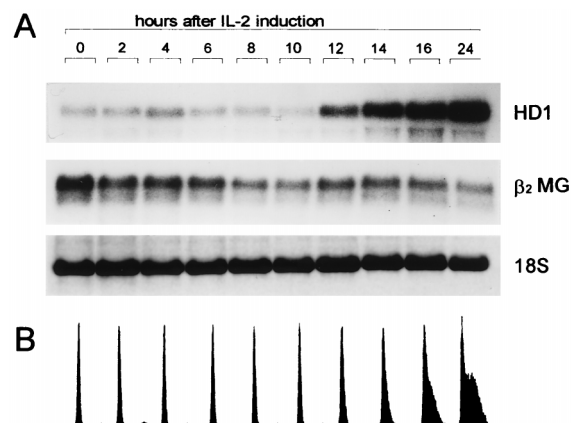


FIG. 5. IL-2 induces HD1 mRNA levels in B6.1 cells. B6.1 cells were arrested by deprivation of IL-2 for 34 h and restimulated for different periods (indicated in hours) with fresh medium containing recombinant IL-2. (A) Cytosolic RNA was analyzed on a Northern blot by sequential hybridization with the radiolabeled HD1 cDNA and a β_2 -microglobulin (β_2 MG) cDNA fragment. To confirm equal loading of RNA, the nylon membrane was stained with methylene blue after transfer to compare the abundance of the 18S rRNA. (B) FACS analysis of DNA content of B6.1 cells during IL-2 stimulation.

sion was not increased further after a prolonged stimulation with IL-2 but stayed constantly high (data not shown). As previously shown (56), levels of β_2 -microglobulin mRNA were not increased upon IL-2 induction of B6.1 cells. In parallel with the RNA extraction, the DNA content of the cells at each stage of growth induction was determined by FACS analysis. As shown in Fig. 5B, B6.1 cells enter S phase at about the same time as HD1 mRNA begins to accumulate in the cytosol of these cells. A similar rise in HD1 mRNA was also observed in both Swiss 3T3 fibroblasts and mouse L cells after serum stimulation of growth-arrested cells (8a).

In a complementary experiment, we wanted to examine the correlation between ongoing growth arrest and the decrease of HD1 mRNA levels in B6.1 cells. Exponentially growing cells were deprived of IL-2, and growth arrest was monitored by FACS analysis (Fig. 6B). As depicted in Fig. 6A, HD1 mRNA expression was high in dividing cells but gradually diminished as the cells arrested in the G_0 phase. The levels of HD1 tran-

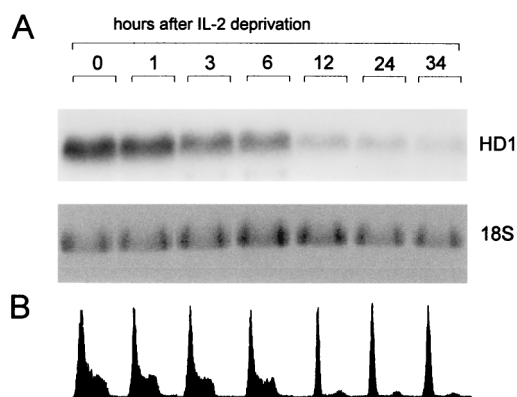


FIG. 6. Decrease of HD1 mRNA expression during IL-2 deprivation. Exponentially growing cells were cultured in complete medium without IL-2 for various times (indicated in hours). (A) Cytosolic RNA was extracted, and HD1 mRNA levels were analyzed by Northern blot hybridization. 18S rRNA was visualized by staining of the nylon membrane with methylene blue. (B) FACS analysis of B6.1 cells during the growth arrest.

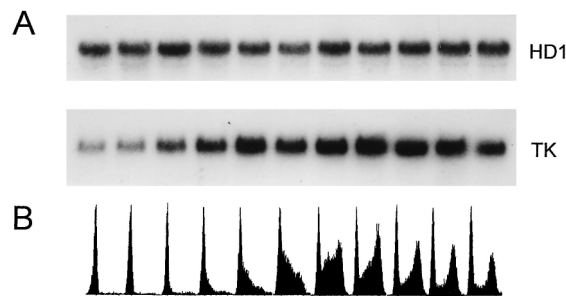


FIG. 7. Cell-cycle-dependent expression of HD1 mRNA. (B) Swiss 3T3 cells were separated according to their size by elutriation, and the cellular DNA content was determined by FACS analysis. (A) Cytosolic RNA was extracted, and equal amounts were analyzed on a Northern blot by hybridization with a radiolabeled HD1 cDNA fragment and as a control with a mouse thymidine kinase (TK) cDNA fragment.

scripts in growth-arrested B6.1 cells were reduced more than fivefold compared to the levels in proliferating cells.

Expression pattern of HD1 mRNA and its regulation during the cell cycle. Next, we investigated if HD1 mRNA expression is not only regulated in response to growth factors but also dependent on the cell cycle phase of proliferating cells. Exponentially growing Swiss 3T3 cells were separated by centrifugal elutriation, and the DNA content of the different fractions was examined by FACS analysis. As shown in Fig. 7, HD1 mRNA levels were unchanged throughout the cell cycle, while thymidine kinase mRNA levels showed, as expected, a significant rise when the cells entered S phase. Therefore, we conclude that HD1 expression, at least at the mRNA level, is constant during the cell cycle of proliferating cells.

Analysis of tissue-specific expression of HD1 by Northern blotting revealed that murine HD1 mRNA was present in all tissues examined, with somewhat reduced levels in liver and a higher abundance in thymus and testis (data not shown). Furthermore, we found a strong overexpression of HD1 transcripts in SV40-transformed kidney cells and in the mouse teratocarcinoma cell line F9, whereas normal HD1 mRNA levels were present in the polyomavirus-transformed cell line COP-8 (unpublished observations).

Mouse HD1 protein is associated with histone deacetylase activity. To examine the expression of endogenous HD1 protein in mouse cells, we raised polyclonal antibodies against a recombinant murine HD1 polypeptide. The HD1 antiserum recognized a single band with the expected size (Fig. 8A, left panel), while the preimmune serum failed to detect specific murine proteins (data not shown). In transfected Swiss 3T3 cells that express a *c-myc*-tagged version of mouse HD1, a second band was detected by the HD1 antiserum. This slightly slower-migrating protein was also recognized by the anti-epitope antibody (Fig. 4A, left panel).

Since the human homolog of HD1 was identified as histone-deacetylating enzyme, we next asked if additional expression of HD1 causes a change in cellular histone deacetylase activity. Whole-cell extracts were prepared from Swiss 3T3 cells expressing epitope-tagged HD1 protein and the untransfected parental cell line and analyzed for histone deacetylase activity. As shown in Fig. 8B, HD activity was significantly higher in transfected cells than in the parental cell line.

To demonstrate a more direct relationship between the presence of HD1 protein and enzyme activity, HD1 protein was immunoprecipitated with the HD1 antiserum from extracts prepared from Swiss 3T3 cells and *c-myc*-HD1-expressing cells. Significant histone deacetylase activity corresponding to about

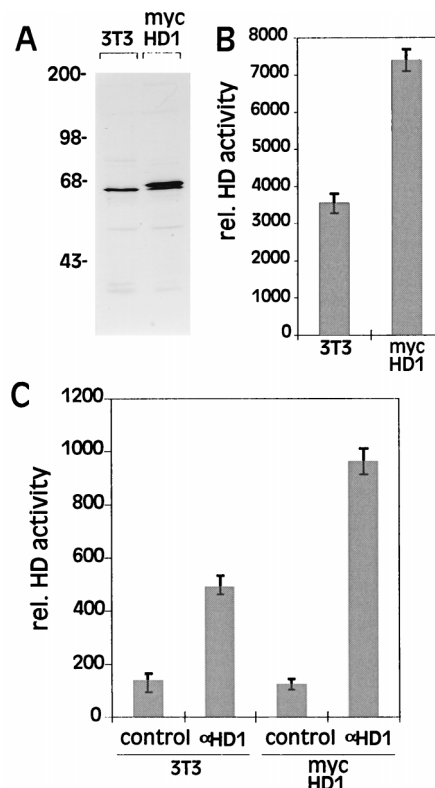


FIG. 8. Histone deacetylase activity is associated with the HD1 protein. Whole-cell extracts were prepared from exponentially growing Swiss 3T3 cells and *c-myc* HD1-expressing cells. (A) Endogenous HD1 protein and epitope-tagged HD1 protein were visualized by immunoblotting with HD1 antiserum. (B) Histone deacetylase activity in the whole-cell extracts was determined in triplicate as described in Materials and Methods and shown as the mean value from triplicate enzyme assays. (C) HD1 was immunoprecipitated, and histone deacetylase activity was determined in aliquots from both immunoprecipitates. In control immunoprecipitations, preimmune serum was used instead of HD1 antiserum.

10% of the input activity was found in immunoprecipitates from both cell lines (Fig. 8C). As expected, the precipitated enzyme activity in the *c-myc*-HD1 cell line was about twofold higher than that in the Swiss 3T3 cells. Furthermore, we were able to precipitate specific histone deacetylase activity in *c-myc*-HD1-expressing cells with the epitope-specific antibody (data not shown). Taken together, these results support the idea that the mouse HD1 protein represents a histone deacetylase.

Growth regulation of cellular histone deacetylase activity and HD1 protein levels in B6.1 cells. In view of the above results, we investigated if cellular histone deacetylase activities change during the growth induction of B6.1 cells. Whole-cell extracts were prepared from IL-2-deprived B6.1 cells and IL-2-stimulated cells and analyzed in HD activity assays. As shown in Fig. 9A, we observed a small but significant increase in histone deacetylase activity after 12 and 24 h of IL-2 induction. To examine if HD1 protein levels are also influenced by IL-2, we analyzed HD1 protein expression during the growth induction of B6.1 cells. By immunoblot analysis, HD1 protein levels were detectable in resting T cells but increased up to sixfold after IL-2 stimulation (Fig. 9B). The induction of HD1 protein occurred with a biphasic kinetics. HD1 protein levels rose threefold during the first 6 h after the addition of IL-2. Since HD1 mRNA expression was unchanged during this period

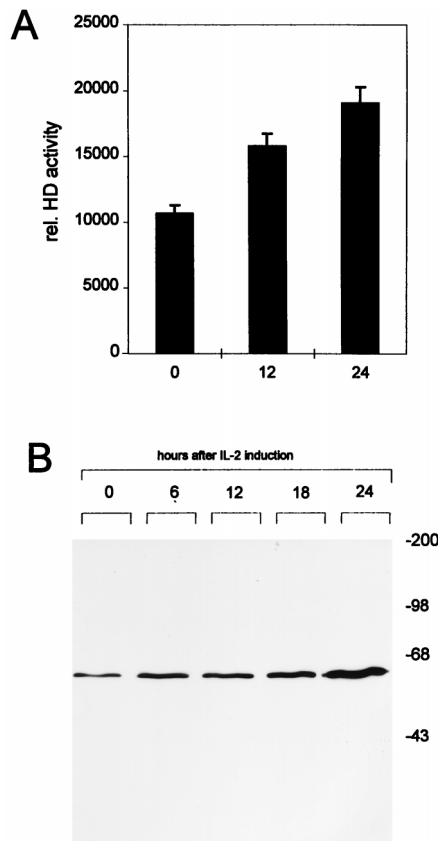


FIG. 9. Cellular histone deacetylase activity and HD1 expression increase upon IL-2 stimulation of B6.1 cells. B6.1 cells were IL-2 deprived, and whole-cell extracts were prepared after different periods of IL-2 stimulation (indicated in hours). (A) Histone deacetylase (HD) activity was determined in triplicate experiments as described in Materials and Methods. The results are depicted as mean values. (B) Equal amounts of protein (50 μ g) were separated on a 10% denaturing sodium dodecyl sulfate-polyacrylamide gel and transferred to a nitrocellulose membrane. HD1 protein was detected on the immunoblot with the monoclonal HD1 antiserum.

(Fig. 5), this increase in HD1 expression seems to be mediated by a posttranscriptional mechanism. When B6.1 cells traversed the S phase, HD1 protein levels increased further, in parallel with the rise in HD1 mRNA levels. These results suggest that enhanced HD1 protein expression in IL-2-stimulated B6.1 cells contributes to the observed rise in total cellular histone deacetylase activity.

HD1 can act as a transcriptional repressor in mammalian cells. Yeast Rpd3 was first identified as a global transcriptional regulator with a primarily negative effect on a number of different genes involved in potassium uptake, methionine metabolism, and mating-type switching (40, 46, 70). To determine whether the mouse HD1 protein also has a negative regulatory function, we analyzed the effect of HD1 expression on an RSV promoter-driven luciferase reporter construct in A549 cells. In previous experiments, this reporter construct had been shown to be inducible by the specific histone deacetylase inhibitor trichostatin A, indicating that the RSV long terminal repeat is sensitive to changes in histone acetylation (data not shown). As shown by the luciferase reporter assays, cotransfection of 0.5 and 1 μ g of pCIneoHD1 resulted in significant concentration-dependent reduction of RSV promoter activity to 60% and less than 25%, respectively, of the control level (Fig. 10). Simultaneous addition of trichostatin A (30 ng/ml) led to a more than

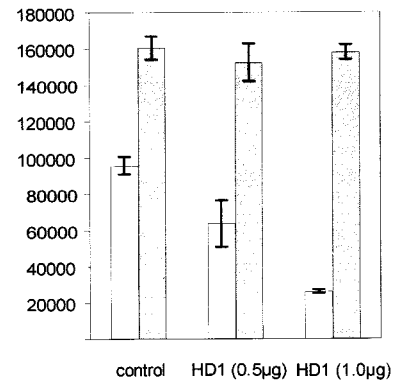


FIG. 10. Negative effect of HD1 on the transcriptional activity of the RSV long terminal repeat. A549 human lung carcinoma cells were transiently transfected with 1 μ g of the reporter plasmid pRSVluc together with 1 μ g of pCIneo (control), with 0.5 μ g of pCIneo plus 0.5 μ g of pCIneoHD1, or with 1 μ g of pCIneoHD1. The cells were cultured for 24 h in the presence (shaded bars) or absence (open bars) of 30 ng of trichostatin A per ml, and luciferase activity was determined as described in Materials and Methods. Relative luciferase activity (in relative light units) is depicted as mean values obtained from triplicate transfections.

fivefold increase in RSV promoter activity despite the presence of coexpressed HD1. We therefore conclude that HD1 can act as a negative regulator of RSV promoter activity in A549 cells.

Overexpression of HD1 leads to a prolongation of the G₂ and M phases in Swiss 3T3 cells. To investigate the effect of HD1 overexpression in more detail, we intended to establish stably transfected Swiss 3T3 cell lines by different transfection methods. However, we were unable to raise G418-resistant clones that express HD1 from the strong cytomegalovirus promoter, suggesting a potential growth-inhibitory effect of the histone-modifying enzyme. To circumvent this problem, mouse HD1 was expressed under the control of the dexamethasone-inducible mouse mammary tumor virus long terminal repeat. Swiss 3T3 cells were stably transfected with pMAMneo or pMAMneoHD1 and analyzed for inducible HD1 overexpression. Two cell lines, HD1-A and HD1-B, representing moderately and strongly HD1-overexpressing Swiss 3T3 cells, respectively, were investigated in more detail. In the absence of dexamethasone, HD1-A cells showed HD1 protein levels that were comparable to that in pMAMneo-transfected control cells (Fig. 11A). Glucocorticoid stimulation of these cells led to about 2.5-fold-increased HD1 levels and to a significant increase in total histone deacetylase activity (Fig. 11A and B). In the presence of dexamethasone, HD1-B cells expressed HD1 proteins at fourfold-higher levels than in Swiss 3T3 cells. The total histone deacetylase activity of these cells was increased threefold compared to that of control cells (Fig. 11B). The slightly elevated HD1 expression in uninduced cells is most probably due some leakiness of the mouse mammary tumor virus promoter in this cell line.

Interestingly, both HD1-overexpressing cell lines showed a remarkable reduction in the growth rate. In the presence of dexamethasone, the doubling times of HD1-A and HD1-B cells were 23 ± 1 and 28 ± 2 h, respectively, compared to 20 ± 1 h for dexamethasone-treated control cells. FACS analysis of HD1-A cells indicated that the portion of G₂/M phase cells increased from 12 to 25% upon treatment with dexamethasone (Fig. 11D). The DNA histogram of pMAMneo-transfected control cells, in contrast, was unchanged after addition of the inducer and similar to the one of uninduced HD1-A cells (data not shown). Removal of dexamethasone from the culture me-

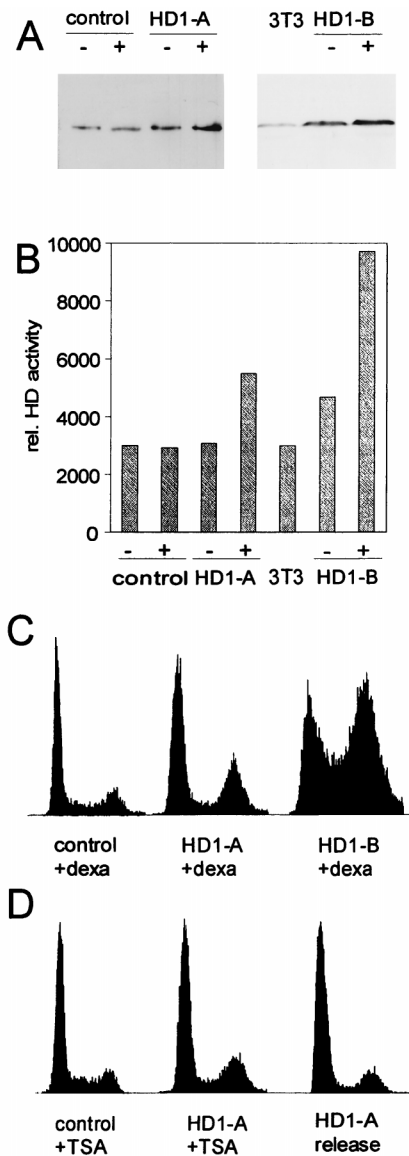


FIG. 11. Effect of HD1 overexpression in Swiss 3T3 fibroblasts. Cells stably transfected with pMAMneo (control) or pMAMneoHD1 (HD1-A and HD1-B) were grown for 4 days in the absence (–) or presence (+) of 1 μ M dexamethasone. (A) Whole-cell extracts were prepared and HD1 protein expression was analyzed by immunoblotting with the HD1 antiserum. (B) Histone deacetylase (HD) activity in the whole-cell extracts was determined as described in Materials and Methods. The data are representative of two independent experiments. (C) DNA histograms of control cells and pMAMneoHD1-transfected cells cultivated with dexamethasone (dexa) as described for panel A. (D) FACS analysis of vector-transfected control cells and HD1-A cells that were exposed to 1 μ M dexamethasone for 4 days. Where indicated, 20 ng of trichostatin A (TSA) per ml was added 24 h prior to harvesting. After 4 days of dexamethasone treatment, one sample of HD1-A cells was further cultivated in medium without the glucocorticoid (release).

dium resulted in a fairly normal cell cycle distribution, indicating that the effect of HD1 is reversible (Fig. 11D, HD1-A release). Furthermore, trichostatin A (20 ng/ml) was able to partially reverse the effect of HD1 overexpression in HD1-A cells. When added to dexamethasone-induced HD1-A cells, the specific histone deacetylase inhibitor reduced the portion of G₂/M phase cells to about 16%, suggesting that the change in cell cycle distribution is linked to histone deacetylase activity

(Fig. 11D). The DNA profile of control cells was unaffected by the same amount of trichostatin A (Fig. 11D). Notably, strongly overexpressing HD1-B cells showed a very unusual cell cycle distribution. About 50% of the total cell population was in the G₂ and M phases of the cell cycle (Fig. 11C). Comparison of the calculated length of the different cell cycle phases indicated that the reduced growth rate of this cell line is due mainly to the drastic prolongation of the G₂ and M phases. Again, treatment with trichostatin A (50 ng/ml) led to a partial reversion of the atypical cell cycle distribution of dexamethasone-induced HD1-B cells (data not shown). When analyzed by fluorescence microscopy, both HD1-overexpressing Swiss 3T3 cell lines showed aberrant cellular and nuclear morphologies, including fragmented nuclei and multiple nuclei per cell, while dexamethasone-treated control cells had a normal morphology. In summary, our results indicate that balanced acetylation and deacetylation of core histones is essential for the undisturbed cell cycle progression of eukaryotic cells.

DISCUSSION

In this paper, we report the isolation and cloning of the murine homolog of the histone deacetylase HD1 as an IL-2-regulated gene. The yeast homolog of HD1 was previously characterized as the yeast transcriptional modulator Rpd3. This protein is required for the maximal induction or repression of a number of regulated yeast genes, including *PHO5*, *TRK2*, *STE6*, *SPO13*, and *HO* (40, 46, 70). The identification of human HD1 as an *RPD3* homolog (65) was therefore a crucial step toward the understanding of the molecular function of this pleiotropic yeast transcriptional regulator. The fact that histone acetylation and deacetylation affect the stability of nucleosomes is in line with the findings that changes in the nucleosomal structures of the promoters of *PHO5* and *STE6* parallel their transcriptional activation (57, 68). However, the regulatory machineries controlling transcription activation in yeast and mammals seem to display significant differences, since murine HD1 failed to fulfill the cellular function of yeast *RPD3*.

The mammalian homolog of Rpd1, another yeast transcription modulator (46, 59, 61), was recently shown to be part of a repressor complex containing both Mad and Max, two proteins involved in the *c-myc* signal transduction pathway (7, 55). Again, the function of *RPD1* in yeast could not be complemented by its mammalian homolog, suggesting that, despite the striking homology, the mammalian protein lacks domains necessary for the interaction with other yeast factors required for transcriptional regulation (22).

We demonstrate here that the murine HD1 is associated with histone-deacetylating activity. A direct relationship between HD1 and histone deacetylation is also underlined by the finding that both transient and inducible expression of HD1 result in a significant increase in enzymatic activity. Given the high homology between the mouse protein and the human histone deacetylase described by Taunton et al. (65), murine HD1 is most probably a histone deacetylase.

Furthermore, we show that HD1 has an inhibitory effect on the transcriptional activity of an RSV enhancer/promoter-driven reporter construct. This result is in good agreement with the recent identification of yet another HD1-related mammalian Rpd3 homolog, mRPD3, as a transcriptional corepressor that interacts with YY1 (73). Transient expression of mRPD3 partially repressed transcription from a promoter containing YY1-binding sites. The repression is significantly enhanced by coexpression of the transcription regulator YY1, indicating

that the recruitment by DNA-binding proteins or complexes is crucial for the cellular function of histone-modifying enzymes. This idea is further supported by recent reports that demonstrate a direct interaction of human HD1 with the retinoblastoma-binding protein p48 (65) and complex formation between the histone acetyltransferase P/CAF and p300, a transcriptional adapter protein involved in cell cycle regulation and differentiation (74). The association of the histone deacetylase with p48 also implies a role for HD1 in the de novo assembly of nucleosomes, since p48 was identified as the small subunit of chromatin assembly factor 1 (69).

We further demonstrate here that HD1 expression in mouse T cells increased after growth stimulation and remained constantly high in exponentially growing cells. The rise in HD1 mRNA and protein levels is paralleled by a significant enhancement of cellular HD activity. These findings imply an important role of histone deacetylation in proliferating cells. Surprisingly, HD1 mRNA and protein expression levels vary up to 10-fold among Swiss 3T3 fibroblasts, B6.1 lymphocytes, and F9 teratocarcinoma cells. The difference in HD1 levels is accompanied by similar variations in cellular histone deacetylase activity (8b). None of these cell lines, however, showed any abnormality in cell cycle progression, suggesting that the activities of different histone-modifying enzymes are regulated in a cell-specific manner. Disturbance of this equilibrium by ectopic overexpression of HD1, however, had serious effects on the growth behavior of transfected Swiss 3T3 cells. Several lines of evidence argue that dynamic changes in the nucleosome structure by histone acetylation and deacetylation are crucial for cell cycle progression of eukaryotic cells. For instance, newly synthesized histones have to undergo acetylation at specific lysine residues but become deacetylated shortly after deposition into the chromatin during the S phase of the cell cycle (see reference 29 for a review). The specific HD inhibitor trichostatin A blocks the proliferation of serum-stimulated fibroblasts in the G₁ phase, whereas cells released from an S phase block arrest in the G₂ phase (76). In yeast cells, removal of the conserved amino terminus of histone H4 causes an increased doubling time with a disproportionately elongated G₂ phase (30). Furthermore, mutational change of the four conserved lysines within that N-terminal domain to arginines is lethal, while substitution by glutamines results in a marked delay during G₁ and G₂/M (41).

It is intriguing that HD1 overexpression in mouse cells leads to a variety of defects similar to the ones that were observed in the genetic analysis of yeast histone H4 mutants. Yeast cells expressing histone variants resembling completely acetylated H4 isoforms had similar phenotypes, including slower growth, delayed progression through the G₂/M phase, and abnormal nuclear morphology (42). Thus, it was suggested that the presence of lysines within the N-terminal H4 domain is required for the maintenance of genome integrity. In mammalian cells, inhibition of histone deacetylation by specific inhibitors and histone deacetylase overexpression had comparable growth-inhibitory effects (31, 76; also see above). This inhibition could be due to an indirect effect on the expression of activators or inhibitors of cell proliferation. Alternatively, changes in the acetylation pattern of nucleosomes could be required for cell cycle progression.

We hypothesize that a reversible modification of histones is equally important for completion of the cell cycle and regulation of gene expression in proliferating cells. The IL-2-dependent upregulation of HD1 expression may simply reflect the need for dynamic changes in the chromatin structure of cycling cells. This model would predict that growth factor-induced cells have an increased turnover of acetyl residues on the

N-terminal histone tails. Detailed studies are under way to determine the kinetics of histone acetylation and deacetylation during IL-2-dependent stimulation of T cells and in HD1-overexpressing cells.

Taken together, our results support the notion that core histone deacetylation constitutes more than a simple trigger for chromatin condensation. Several distinct acetyltransferases and deacetylases have 24 to 28 lysine residues per nucleosome as potential targets for modification. The situation is further complicated by the possible modulation of these enzymes by accessory proteins like Sin3, YY1, or the Rb-binding protein p48. We therefore believe that both acetylating and deacetylating activities are involved in the regulation of gene expression. Subtle but significant variations in the acetylation pattern of core histones could not only change chromatin structures but also modulate the affinity of *trans*-acting factors. The characterization of these proteins, together with the identification of factors interacting with histone-modifying enzymes, should allow us to unravel the underlying mechanisms.

ACKNOWLEDGMENTS

We thank M. Nabholz for the B6.1 cell line and recombinant IL-2, T. Sauer for expert technical assistance with the flow cytometry, S. Brunner for Swiss 3T3 cell cycle and mouse tissue Northern blots, M. Cotten for providing the pRSVluc plasmid and A549 cells, S. Chiocca for help with the luciferase assays, A. Kranawetter for the photographs, R. Hofbauer for the 3T3 cDNA library, and members of K. Kuchler's laboratory for helpful suggestions concerning the yeast work. We are grateful to R. Gaber for providing yeast strains, to the P. Loidl laboratory for providing labeled histones, to E. W. Muellner for supplying the 28S probe, and to P. Loidl, E. W. Muellner, and M. Nabholz for critical comments on the manuscript. We thank E. Ogris and P. Loidl for many encouraging discussions.

K.K. was supported by funds from the Austrian Science Foundation project MOB-10123. The work in the C.S. laboratory was supported by grants from the Austrian Ministry of Science (70.003/2-Pr/4/95), the Austrian Science Foundation project GEN-11179, and the Anniversary Fund of the Austrian National Bank. J.T. is a fellow of the Vienna Biocenter Ph.D. program.

S. Bartl and J. Taplick contributed equally to this work.

REFERENCES

- Adamczewski, J. P., J. V. Gannon, and T. Hunt. 1993. Simian virus 40 large T antigen associates with cyclin A and p33cdk2. *J. Virol.* **67**:6551-6557.
- Almouzni, G., S. Khochbin, S. Dimitrov, and A. P. Wolffe. 1994. Histone acetylation influences both gene expression and development of *Xenopus laevis*. *Dev. Biol.* **165**:654-669.
- Alonso, W. R., and D. A. Nelson. 1986. A novel yeast histone deacetylase: partial characterization and development of an activity assay. *Biochim. Biophys. Acta* **866**:161-169.
- Annunziato, A. T., and R. L. Seale. 1983. Histone deacetylation is required for the maturation of newly replicated chromatin. *J. Biol. Chem.* **258**:12675-12684.
- Arts, J., M. Lansink, J. Grimbergen, K. H. Toet, and T. Kooistra. 1995. Stimulation of tissue-type plasminogen activator gene expression by sodium butyrate and trichostatin A in human endothelial cells involves histone acetylation. *Biochem. J.* **310**:171-176.
- Attisano, L., and P. N. Lewis. 1990. Purification and characterization of two porcine liver nuclear histone acetyltransferases. *J. Biol. Chem.* **265**:3949-3955.
- Ayer, D. E., Q. A. Lawrence, and R. N. Eisenman. 1995. Mad-Max transcriptional repression is mediated by ternary complex formation with mammalian homologs of yeast repressor Sin3. *Cell* **80**:767-776.
- Ballester, R., T. Michaeli, K. Ferguson, H. P. Xu, F. McCormick, and M. Wigler. 1989. Genetic analysis of mammalian GAP expressed in yeast. *Cell* **59**:681-686.
- Bartl, S. Unpublished observations.
- Bartl, S., et al. Unpublished observations.
- Belikoff, E., L. J. Wong, and B. M. Alberts. 1980. Extensive purification of histone acetylase A, the major histone N-acetyl transferase activity detected in mammalian cell nuclei. *J. Biol. Chem.* **255**:11448-11453.
- Bradbury, E. M. 1992. Reversible histone modifications and the chromosome cell cycle. *Bioessays* **14**:9-16.

11. Braunstein, M., A. B. Rose, S. G. Holmes, C. D. Allis, and J. R. Broach. 1993. Transcriptional silencing in yeast is associated with reduced nucleosome acetylation. *Genes Dev.* **7**:592–604.
12. Brosch, G., R. Ransom, T. Lechner, J. D. Walton, and P. Loidl. 1995. Inhibition of maize histone deacetylases by HC toxin, the host-selective toxin of *Cochliobolus carbonum*. *Plant Cell* **7**:1941–1950.
13. Brownell, J. E., J. Zhou, T. Ranalli, R. Kobayashi, D. G. Edmondson, S. Y. Roth, and C. D. Allis. 1996. *Tetrahymena* histone acetyltransferase A: a homolog to yeast Gcn5p linking histone acetylation to gene activation. *Cell* **84**:843–851.
14. de Wet, J. R., K. V. Wood, M. DeLuca, D. R. Helinski, and S. Subramani. 1987. Firefly luciferase gene: structure and expression in mammalian cells. *Mol. Cell. Biol.* **7**:725–737.
15. Egner, R., Y. Mahé, R. Pandjaitan, and K. Kuchler. 1995. Endocytosis and vacuolar degradation of the plasma membrane-localized Pdr5 ATP-binding cassette multidrug transporter in *Saccharomyces cerevisiae*. *Mol. Cell. Biol.* **15**:5879–5887.
16. Evan, G. I., G. K. Lewis, G. Ramsay, and J. M. Bishop. 1985. Isolation of monoclonal antibodies specific for human *c-myc* proto-oncogene product. *Mol. Cell. Biol.* **5**:3610–3616.
17. Futamura, M., Y. Monden, T. Okabe, J. Fujita Yoshigaki, S. Yokoyama, and S. Nishimura. 1995. Trichostatin A inhibits both ras-induced neurite outgrowth of PC12 cells and morphological transformation of NIH3T3 cells. *Oncogene* **10**:1119–1123.
18. Garcea, R. L., and B. M. Alberts. 1980. Comparative studies of histone acetylation in nucleosomes, nuclei, and intact cells. Evidence for special factors which modify acetylase action. *J. Biol. Chem.* **255**:11454–11463.
19. Georgieva, E. I., G. Lopez Rodas, R. Sendra, P. Grobner, and P. Loidl. 1991. Histone acetylation in *Zea mays*. II. Biological significance of post-translational histone acetylation during embryo germination. *J. Biol. Chem.* **266**:18751–18760.
20. Girardot, V., T. Rabilloud, M. Yoshida, T. Beppu, J. J. Lawrence, and S. Khochbin. 1994. Relationship between core histone acetylation and histone H1(0) gene activity. *Eur. J. Biochem.* **224**:885–892.
21. Grabher, A., G. Brosch, R. Sendra, T. Lechner, E. Eberharther, E. I. Georgieva, G. Lopez Rodas, L. Franco, H. Dietrich, and P. Loidl. 1994. Subcellular location of enzymes involved in core histone acetylation. *Biochemistry* **33**:14887–14895.
22. Halleck, M. S., S. Pownall, K. W. Harder, A. M. Duncan, F. R. Jirik, and R. A. Schlegel. 1995. A widely distributed putative mammalian transcriptional regulator containing multiple paired amphipathic helices, with similarity to yeast SIN3. *Genomics* **26**:403–406.
23. Hay, C. W., and E. P. Candido. 1983. Histone deacetylase. Association with a nuclease resistant, high molecular weight fraction of HeLa cell chromatin. *J. Biol. Chem.* **258**:3726–3734.
24. Hofbauer, R., E. Mullner, C. Seiser, and E. Wintersberger. 1987. Cell cycle regulated synthesis of stable mouse thymidine kinase mRNA is mediated by a sequence within the cDNA. *Nucleic Acids Res.* **15**:741–752.
25. Hoshikawa, Y., H. J. Kwon, M. Yoshida, S. Horinouchi, and T. Beppu. 1994. Trichostatin A induces morphological changes and gelsolin expression by inhibiting histone deacetylase in human carcinoma cell lines. *Exp. Cell Res.* **214**:189–197.
26. Inoue, A., and D. Fujimoto. 1970. Histone deacetylase from calf thymus. *Biochim. Biophys. Acta* **220**:307–316.
27. Jeppesen, P., and B. M. Turner. 1993. The inactive X chromosome in female mammals is distinguished by a lack of histone H4 acetylation, a cytogenetic marker for gene expression. *Cell* **74**:281–289.
28. Jones, J. S., and L. Prakash. 1990. Yeast *Saccharomyces cerevisiae* selectable markers in pUC18 polylinkers. *Yeast* **6**:363–366.
29. Kaufman, P. D. 1996. Nucleosome assembly: the CAF and the HAT. *Curr. Opin. Cell Biol.* **8**:369–373.
30. Kayne, P. S., U. J. Kim, M. Han, J. R. Mullen, F. Yoshizaki, and M. Grunstein. 1988. Extremely conserved histone H4 N terminus is dispensable for growth but essential for repressing the silent mating loci in yeast. *Cell* **55**:27–39.
31. Kijima, M., M. Yoshida, K. Sugita, S. Horinouchi, and T. Beppu. 1993. Trapoxin, an antitumor cyclic tetrapeptide, is an irreversible inhibitor of mammalian histone deacetylase. *J. Biol. Chem.* **268**:22429–22435.
32. Kleff, S., E. D. Andrulis, C. W. Anderson, and R. Sternglanz. 1995. Identification of a gene encoding a yeast histone H4 acetyltransferase. *J. Biol. Chem.* **270**:24674–24677.
33. Lechner, T., A. Lusser, G. Brosch, A. Eberharther, M. Goralik Schramel, and P. Loidl. 1996. A comparative study of histone deacetylases of plant, fungal and vertebrate cells. *Biochim. Biophys. Acta* **1296**:181–188.
34. Liang, P., and A. B. Pardee. 1992. Differential display of eukaryotic messenger RNA by means of the polymerase chain reaction. *Science* **257**:967–971.
35. Loidl, P. 1994. Histone acetylation: facts and questions. *Chromosoma* **103**:441–449.
36. Loidl, P. 1988. Towards a understanding of the biological function of histone acetylation. *FEBS Lett.* **227**:91–95.
37. Lopez Rodas, G., G. Brosch, G. Golderer, H. Lindner, P. Grobner, and P. Loidl. 1992. Enzymes involved in the dynamic equilibrium of core histone acetylation of *Physarum polycephalum*. *FEBS Lett.* **296**:82–86.
38. Lopez Rodas, G., E. I. Georgieva, R. Sendra, and P. Loidl. 1991. Histone acetylation in *Zea mays*. I. Activities of histone acetyltransferases and histone deacetylases. *J. Biol. Chem.* **266**:18745–18750.
39. Lopez Rodas, G., V. Tordera, M. M. Sanchez del Pino, and L. Franco. 1989. Yeast contains multiple forms of histone acetyltransferase. *J. Biol. Chem.* **264**:19028–19033.
40. McKenzie, E. A., N. A. Kent, S. J. Dowell, F. Moreno, L. E. Bird, and J. Mellor. 1993. The centromere and promoter factor, 1, CPF1, of *Saccharomyces cerevisiae* modulates gene activity through a family of factors including SPT21, RPD1 (SIN3), RPD3 and CCR4. *Mol. Genet.* **240**:374–386.
41. Megee, P. C., B. A. Morgan, B. A. Mittman, and M. M. Smith. 1990. Genetic analysis of histone H4: essential role of lysines subject to reversible acetylation. *Science* **247**:841–845.
42. Megee, P. C., B. A. Morgan, and M. M. Smith. 1995. Histone H4 and the maintenance of genome integrity. *Genes Dev.* **9**:1716–1727.
43. Miyashita, T., H. Yamamoto, Y. Nishimune, M. Nozaki, T. Morita, and A. Matsushiro. 1994. Activation of the mouse cytokeratin A (endo A) gene in teratocarcinoma F9 cells by the histone deacetylase inhibitor Trichostatin A. *FEBS Lett.* **353**:225–229.
44. Mold, D. E., and K. S. McCarty, Sr. 1987. A Chinese hamster ovary cell histone deacetylase that is associated with a unique class of mononucleosomes. *Biochemistry* **26**:8257–8262.
45. Morgenstern, J. P., and H. Land. 1990. Advanced mammalian gene transfer: high titre retroviral vectors with multiple drug selection markers and a complementary helper-free packaging cell line. *Nucleic Acids Res.* **18**:3587–3596.
46. Nasmyth, K., D. Stillman, and D. Kipling. 1987. Both positive and negative regulators of HO transcription are required for mother-cell-specific mating-type switching in yeast. *Cell* **48**:579–587.
47. O'Neill, L., and B. M. Turner. 1995. Histone H4 acetylation distinguishes coding regions of the human genome from heterochromatin in a differentiation-dependent but transcription-independent manner. *EMBO J.* **14**:3946–3957.
48. Pear, W. S., G. P. Nolan, M. L. Scott, and D. Baltimore. 1993. Production of high-titer helper-free retroviruses by transient transfection. *Proc. Natl. Acad. Sci. USA* **90**:8392–8396.
49. Perry, C. A., and A. T. Annunziato. 1991. Histone acetylation reduces H1-mediated nucleosome interactions during chromatin assembly. *Exp. Cell Res.* **196**:337–345.
50. Pesis, K. H., and H. R. Matthews. 1986. Histone acetylation in replication and transcription: turnover at specific acetylation sites in histone H4 from *Physarum polycephalum*. *Arch. Biochem. Biophys.* **251**:665–673.
51. Ramanathan, B., and M. J. Smerdon. 1989. Enhanced DNA repair synthesis in hyperacetylated nucleosomes. *J. Biol. Chem.* **264**:11026–11034.
52. Rose, M. D., F. Winston, and P. Hieter. 1990. Methods in yeast genetics. A laboratory course manual. Cold Spring Harbor Laboratory Press, Cold Spring Harbor, N.Y.
53. Rothstein, R. J. 1983. One-step gene disruption in yeast. *Methods Enzymol.* **101**:202–211.
54. Rundlett, S. E., A. A. Carmen, R. Kobayashi, S. Bavykin, B. M. Turner, and M. Grunstein. 1996. HDA1 and RPD3 are members of distinct yeast histone deacetylase complexes that regulate silencing and transcription. *Proc. Natl. Acad. Sci. USA* **93**:14503–14508.
55. Schreiber Agus, N., L. Chin, K. Chen, R. Torres, G. Rao, P. Guida, A. I. Skoultschi, and R. A. DePino. 1995. An amino-terminal domain of Mx1 mediates anti-Myc oncogenic activity and interacts with a homolog of the yeast transcriptional repressor SIN3. *Cell* **80**:777–786.
56. Seiser, C., S. Teixeira, and L. C. Kuhn. 1993. Interleukin-2-dependent transcriptional and post-transcriptional regulation of transferrin receptor mRNA. *J. Biol. Chem.* **268**:13074–13080.
57. Shimizu, M., S. Y. Roth, C. Szent Gyorgyi, and R. T. Simpson. 1991. Nucleosomes are positioned with base pair precision adjacent to the alpha 2 operator in *Saccharomyces cerevisiae*. *EMBO J.* **10**:3033–3041.
58. Smith, P. J. 1986. n-Butyrate alters chromatin accessibility to Dna repair enzymes. *Carcinogenesis* **7**:423–429.
59. Sternberg, P. W., M. J. Stern, I. Clark, and I. Herskowitz. 1987. Activation of the yeast HO gene by release from multiple negative controls. *Cell* **48**:567–577.
60. Strebhardt, K., J. I. Mullins, C. Bruck, and H. Rubsamen Waigmann. 1987. Additional member of the protein-tyrosine kinase family: the *src*- and *lck*-related protooncogene *c-tkl*. *Proc. Natl. Acad. Sci. USA* **84**:8778–8782.
61. Strich, R., M. R. Slater, and R. E. Esposito. 1989. Identification of negative regulatory genes that govern the expression of early meiotic genes in yeast. *Proc. Natl. Acad. Sci. USA* **86**:10018–10022.
62. Sugita, K., K. Koizumi, and H. Yoshida. 1992. Morphological reversion of sis-transformed NIH3T3 cells by trichostatin A. *Cancer Res.* **52**:168–172.
63. Sutterluety, H., S. Bartl, J. Karlseder, E. Wintersberger, and C. Seiser. 1996. Carboxy-terminal residues of mouse thymidine kinase are essential for the rapid degradation in quiescent cells. *J. Mol. Biol.* **259**:383–392.
64. Talasz, H., G. Weiss, and B. Puschendorf. 1990. Replication-linked histone

- acetylation in rat liver tissue is sensitive to alkylating agents. FEBS Lett. **264**:141–144.
65. **Taunton, J., C. A. Hassig, and S. L. Schreiber.** 1996. A mammalian histone deacetylase related to the yeast transcriptional regulator Rpd3p. *Science* **272**:408–411.
66. **Travis, G. H., M. Colavito Shepanski, and M. Grunstein.** 1984. Extensive purification and characterization of chromatin-bound histone acetyltransferase from *Saccharomyces cerevisiae*. *J. Biol. Chem.* **259**:14406–14412.
67. **Turner, B. M., A. J. Birley, and J. Lavender.** 1992. Histone H4 isoforms acetylated at specific lysine residues define individual chromosomes and chromatin domains in *Drosophila* polytene nuclei. *Cell* **69**:375–384.
68. **Venter, U., J. Svaren, J. Schmitz, A. Schmid, and W. Horz.** 1994. A nucleosome precludes binding of the transcription factor Pho4 in vivo to a critical target site in the PHO5 promoter. *EMBO J.* **13**:4848–4855.
69. **Verreault, A., P. D. Kaufman, R. Kobayashi, and B. Stillman.** 1996. Nucleosome assembly by a complex of CAF-1 and acetylated histones H3/H4. *Cell* **87**:95–104.
70. **Vidal, M., and R. F. Gaber.** 1991. *RPD3* encodes a second factor required to achieve maximum positive and negative transcriptional states in *Saccharomyces cerevisiae*. *Mol. Cell. Biol.* **11**:6317–6327.
71. **von Boehmer, H., H. Hengartner, M. Nabholz, W. Lernhardt, M. H. Schreier, and W. Haas.** 1979. Fine specificity of a continuously growing killer cell clone specific for H-Y antigen. *Eur. J. Immunol.* **9**:592–597.
72. **Wolffe, A. P.** 1994. Transcription: in tune with the histones. *Cell* **77**:13–16.
73. **Yang, W.-M., C. Inouye, Y. Zeng, D. Bearss, and E. Seto.** 1996. Transcriptional repression by YY1 is mediated by interaction with a mammalian homolog of the yeast global regulator RPD3. *Proc. Natl. Acad. Sci. USA* **93**:12845–12850.
74. **Yang, X.-J., V. V. Ogryzko, J. Nishikawa, B. H. Howard, and Y. Nakatani.** 1996. A p300/CBP-associated factor that competes with the adenoviral oncoprotein E1A. *Nature* **382**:319–324.
75. **Yoshida, H., and K. Sugita.** 1992. A novel tetracyclic peptide, trapoxin, induces phenotypic change from transformed to normal in sis-oncogene-transformed NIH3T3 cells. *Jpn. J. Cancer Res.* **83**:324–328.
76. **Yoshida, M., and T. Beppu.** 1988. Reversible arrest of proliferation of rat 3Y1 fibroblasts in both the G1 and G2 phases by trichostatin A. *Exp. Cell Res.* **177**:122–131.
77. **Yoshida, M., S. Horinouchi, and T. Beppu.** 1995. Trichostatin A and trapoxin: novel chemical probes for the role of histone acetylation in chromatin structure and function. *Bioessays* **17**:423–430.
78. **Yoshida, M., S. Nomura, and T. Beppu.** 1987. Effects of trichostatins on differentiation of murine erythroleukemia cells. *Cancer Res.* **47**:3688–3691.